Penerbit Akademia Baru

CFD Letters

Journal homepage: www.akademiabaru.com/cfdl.html
ISSN: 2180-1363

CFD Study On the Behaviour and Turbulence of the Airflow Induced by The Moving Elevator Car in Elevator Shaft Using K-Epsilon Model

Open Access

Jia Hui Ang[1], Yusri Yusup[1], Sheikh Ahmad Zaki[2], Ali Salehabadi[1], Mardiana Idayu Ahmad[1,*]

[1] Environmental Technology Division, School of Industrial Technology, Universiti Sains Malaysia, 11800 Penang, Malaysia
[2] Department of Mechanical Precision Engineering, Malaysia-Japan International Institute of Technology, Universiti Teknologi Malaysia, 54100 Kuala Lumpur, Malaysia

ARTICLE INFO

Article history:
Received 19 September 2019
Received in revised form 14 November 2019
Accepted 10 November 2019
Available online 27 November 2019

ABSTRACT

Land scarcity in relation to the swift urbanisation causes vertical development of buildings and infrastructures. The increasing importance of the main vertical transport - elevator, urges the elevator aerodynamics study to evaluate its acoustic, ride comfort, aerodynamics performance, and airflow effect. They were carried out experimentally or(and) via modeling and simulation. However, among the very limited published CFD studies on the elevator aerodynamics, there is insufficient detailed method and data been presented. Consequently, there is a very limited open-source established method and preliminary data necessary for the elevator aerodynamic study, restricting the potential improvement in this topic. Therefore, this paper studies the behaviour and turbulence of the airflow induced by the elevator car movement in the elevator shaft using the PIMPLE algorithm and the k-epsilon model. Details on the theories and methods were explained and discussed, which include the computational domain settings, governing principles and equations, numerical methods and mechanisms, and boundary conditions. An unsteady, turbulent, incompressible, and Newtonian airflow was assumed in the OpenFOAM simulation. The airflow was affected mainly by the blockage effect and the Bernoulli's effect. The simulation result obeys the theories of fluid mechanics and physics, indicating its reliability to be the preliminary data for further study.

Keywords:
CFD; elevator system; PIMPLE algorithm; k-epsilon turbulence model; OpenFoam

1. Introduction

Rapid development, population growth, and land scarcity lead to the vertical development of buildings and infrastructures. Along with the increasing demand for vertical transport, aerodynamics study on the elevator system is increasingly important to evaluate the acoustic, ride comfort, aerodynamics performance, airflow effect of the elevator movement, as well as the potential of kinetic energy harvesting [1–6]. The earlier elevator aerodynamics studies were carried out based on experiments only. For example, Hisashi *et al.,* [7] carried out the study using the oil flow pattern

* *Corresponding author.*
E-mail address: mardianaidayu@usm.my (Mardiana Idayu Ahmad)

technique and wind tunnel method to visualize and determine the pressure fluctuation distribution respectively. Modeling and simulation were emerging to better study the aerodynamics of the elevator by determining the significant measurement area and to extrapolate the inaccessible conditions of experimental studies based on the initial input. Many studies use the new or past experimental data as a guide to develop valid modeling and simulation set up and then solve the numerical equations to produce the extrapolated results. At the earlier stage of modeling and simulation technology, Hisashi [8] studied on the aerodynamics-induced acoustic effect of the apron to the flow around the car using both experiments and numerical simulation. The experiments were only used for visualization, while the numerical simulation provides quantitative results. Positively, the advancement of technology enables a more accurate and comprehensive quantitative experimental study, as well as a faster, realistic and flexible modeling and simulation of the airflow. For example, the study on the effect of blockage ratio on the performance of high-speed elevator by Wang *et al.,* [9] using computational fluid dynamics (CFD) software reduce its computational cost using a quarter model.

Naiver-Stokes equation and its derivatives are the main governing equations for the aerodynamics studies. For the modeling and simulation using CFD software, different numerical solvers and turbulence models were used based on the objective of the study. PIMPLE algorithm was preferable for the unsteady incompressible turbulent flow. Modeling and simulation approaches of Reynolds Average Naiver-Stokes (RANS) and Detached Eddies Simulation (DES) were commonly used in the past studies on elevator aerodynamics. There are several turbulence models classified based on the modeling and simulation approaches, for example, the k-epsilon model and the k-omega model are under RANS, whereas the k-omega Shear Stress Transport (SST) model is under DES [10].

The standard k-epsilon model is suitable to be applied for high Reynolds number case. The application of wall function skips the necessity of the simulation of the buffer region in order to save the computational cost. This model is linear so has fast convergence and low memory demand, but it is less accurate when there is an adverse pressure gradient, strong curvature or jet flow. It is suitable for the flow with consistent pressure from inlet to outlet, and external flow around complex geometries bluff body. It provides a good initial guess for preliminary study before using other more complicated models or carrying out experiments [11-12]. The low Reynolds k-epsilon does not apply wall function, so it requires a denser mesh. It is usually used after getting the initial guess value from the preliminary study using the standard k-epsilon model, in order to simulate the problem more accurately. For the case to study the overall airflow within the elevator system, the k-epsilon turbulence model was used. For example, the study on flow effect to ride comfort, and the aerodynamics performance of the elevator car [13-14].

The k-omega model is suitable for low Reynolds number flow yet the wall function can be applied. It is non-linear thus has a slower convergence. It is sensitive to the initial condition value, so it requires the preliminary study using a less sensitive model such as k-epsilon to obtain initial guess values. K-omega is accurate for internal flow, and flow with strong curvature, separated flow, and jet flow. For the case to focus near-wall interaction for smaller scale eddies, the k-omega turbulence model was used [4,9,15]. For example, the studies on the small scale eddies, which contribute to the aero-vibroacoustic factor were done to evaluate the lateral aerodynamic buffeting effects [15].

The advancement of the CFD solving method combines k-epsilon and k-omega as k-omega SST, using the appropriate model based on the location of the problem, which is the k-epsilon for the free stream far from the wall, and the k-omega for the near-wall flow. Its resolution is equal to that of the k-omega and the low Reynolds number k-epsilon but without the weakness of the pure k-epsilon and k-omega [11]. The k-omega SST provides an accurate initial guess as to the k-epsilon, and simulate flow separation in adverse pressure gradient conditions as the k-omega. The past study on Fluid-

Structure Interaction (FSI) using k-omega SST was done by Singh *et al.,* [16] to analyze the airflow effect within the elevator system.

Nevertheless, there are limited published studies on the behaviour and turbulence of the airflow induced by the moving elevator car using CFD. A point often overlooked, is that most of these past studies did not discuss the solving principles and methods of numerical solvers (algorithms) and turbulence models used in detail. Many studies on aero-vibro and acoustic factors of the elevator system did not specify the type of the numerical solver and turbulence model used [3,17–19]. Consequently, there is a very limited open-source established method to guide the elevator aerodynamics studies, causing less exploration in this topic. Moreover, the preliminary data necessary for the experimental study as well as advanced modelling and simulation of the elevator car in the shaft are scarce. This restricts the potential improvement in the aerodynamics of the elevator car thus far.

Therefore, this paper studies the behaviour and turbulence of the airflow induced by the elevator car movement in the elevator shaft using the PIMPLE algorithm and the k-epsilon model. Details on the numerical algorithm and turbulence model were explained and discussed, which include the computational domain settings, governing principles and equations, numerical methods and mechanisms, and boundary conditions. This study can determine the significant measurement points in a wind tunnel experiment as well as provide initial guess value to be input into the modeling and simulation using k-omega and k-omega SST.

2. Methodology

Pre-processing was done using Salome, meshing and solving were done using OpenFOAM, while post-processing was done using Paraview.

2.1 Computational Domain and Set Up

The symmetry quarter of the elevator system was modeled to represent the elevator system. The computational domain meshed into grids consisting of 142527 cells, which are 141897 hexahedra and 630 polyhedra. Figure 1 shows the computational domain of the elevator system, which uses the static mesh approach. The downward movement of the elevator car at 10 m s^{-1} within the shaft was represented by the air inflow and outflow from the base of the shaft and top of shaft respectively at 10 m s^{-1}. Simulation period of 20 s with the time steps interval 0.003125 s was used since the preliminary test shows its sufficiency for the flow to be stable with a relatively constant parameter value and flow pattern.

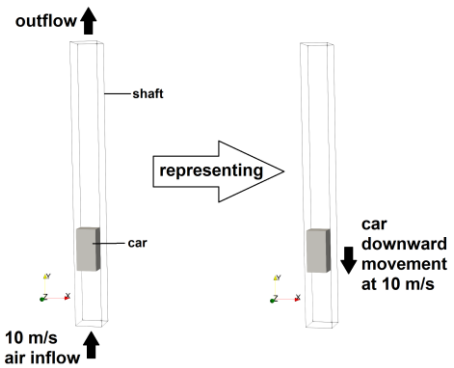

Fig. 1. Computational domain of the elevator system

2.2 Numerical Algorithm: PIMPLE Algorithm

The atmospheric pressure and air density reduction can be neglected since most of the elevator shaft in high-rise buildings is less than 500 m [20-21]. Another point is that the elevator car is moving at only 10 m/s, which is less than the speed of sound (340 m/s). The induced airflow has insufficient energy to compress the air within the shaft. Moreover, most of the HVAC system in typical buildings maintains the air properties at the ambient air condition [22]. In that case, incompressible flow is assumed in this study. Since there is no strong thermal source in the elevator shaft, the air within it is assumed as a Newtonian fluid, which has a constant viscosity of 1.864 X 10^{-5}. The unsteady turbulent incompressible Newtonian viscous flow induced by the elevator car movement is governed by the continuity equation, time-averaged Navier-Stokes equations (Reynolds Average Navier-Stokes equations), and modified k-epsilon turbulence model equations. These equations work based on the conservation of mass and momentum, with constant air temperature and thus constant density and viscosity. Parameters simulated are air velocity in three directions, U_x, U_y, U_z; kinematic static pressure, p; turbulent kinetic energy, k and dissipation rate of turbulent kinetic energy, ϵ.

PIMPLE algorithm assumes an unsteady, incompressible, viscous and Newtonian flow. The simplified incompressible Navier-Stokes equations governing the PIMPLE algorithm are as in Eqs. (1) and (2). These equations are input with the boundary conditions and initial conditions, as well as the turbulence parameters to solve a case.

$$\nabla \cdot u = 0 \tag{1}$$

$$\frac{d}{dt}u + \nabla \cdot (uu) + \left(v_{eff}\nabla^2 u\right) = -\nabla p \tag{2}$$

Where u is the velocity (m s^{-1}), p is the kinematic static pressure (m s^{-2}), and v_{eff} is the effective kinematic viscosity.

It is the combination of the PISO and the SIMPLE algorithm. Initially, it uses the SIMPLE algorithm to initiate the flow and determine the guess value for the following simulation. It uses the SIMPLE steady-state treatment to compute the steady-state solution for each time step, which enables the Courant number to be larger than one. However, it solves the weakness of the SIMPLE algorithm in neglection of transient behaviour and development of flow, which is caused by its large time step. It enables a larger time step yet maintaining the accuracy and accounting of temporal change as in the PISO algorithm. This enables it to reduce the computational cost while accounting for the significant transient behaviour and development of flow. Consequently, the higher computational cost of each time step is needed but a larger time step is allowed in the PIMPLE algorithm. It is compatible with all turbulence models in the OpenFOAM software.

It works based on the parameters of velocity, u (m s^{-1}) and kinematic pressure, P (m^2 s^{-2}), which are input into the mechanism of pressure-momentum coupling with the following steps. Firstly, a momentum matrix is constructed using the guess value, then the pressure matrix is constructed based on this momentum matrix, and pressure is calculated. The velocity initial guess value is corrected with the newly calculated pressure value. The momentum matrix is then reconstructed using the new velocity value. The whole cycle is repeated again until the adjustment of the velocity. The number of cycles (loops) per time step depends on the nOuterCorrector set, which is usually 2. PIMPLE algorithm stabilizes the simulation using the relaxation factor by mixing the current result with the previous one in between each time step to smoothen the convergence rate. It also moderates the convergence rate using residual control and nOuterCorrector.

2.3 Turbulence Model: k-epsilon Model

k-epsilon model was used in this study since it is suitable to be applied in the case with high Reynolds (Re) and turbulence flow, which its pressure gradient from inlet to outlet is low [12]. Although it has a lower fidelity of the near-wall region, it is sufficient for this study, which aims to study the overall airflow within the elevator system. The results are sufficient to be used to determine the high velocity and low turbulence points, acting as the preliminary guide for experimental studies such as wind tunnel, as well as the initial guess to be input to a higher-order accuracy solving approaches or resolutions. This study only involves study on a big section of the shaft instead of focusing on the specific near-wall region. Low turbulence k-epsilon and k-omega will be used for further study after got the baseline study done using k-epsilon.

k-epsilon model is a two-equation model with parameters of turbulence kinetic energy, k ($m^2 s^{-2}$); and turbulence dissipation rate, ϵ. k is the kinetic energy per unit mass of the turbulent fluctuations in a turbulent airflow. ϵ is the rate of dissipation of k. For the Newtonian fluid, it is the decrement of the k because the energy was used to fluctuate the viscous stresses that resist the change of the fluid by the fluctuating strain rates [23]. It uses wall functions, which are kqRWallFunction and epsilonWallFunction to reduce the computational cost for the near-wall region. For the isotropic turbulence, the initial value of parameters can be estimated using the established formula as in Eqs. (3) to (5) [24-25].

$$k = 3/2\ (uI)^2 \tag{3}$$

Where
u is the air velocity ($m\ s^{-1}$)
I is the turbulence intensity

$$\epsilon = C_\mu^{\frac{3}{4}} \frac{k^{\frac{3}{2}}}{l} \tag{4}$$

Where
C_μ is the k epsilon model constant which typically valued as 0.09
k is the turbulence kinetic energy ($m\ s^{-2}$)
l is the turbulence or eddy length scale

$$l = 0.07\ L \tag{5}$$

Where
L is the characteristic length of the case

2.3.1 Standard k-epsilon model equations

Eqs. (6) to (8) show the equations of the standard k-epsilon model, namely equation of k, equation of ϵ, and equation of turbulence viscosity respectively [26-27]. Most of the CFD software uses these equations with the default value of the coefficients as shown in Table 1. However, some software such as OpenFOAM uses the modified equations of the k-epsilon model.

$$\frac{D}{Dt}(\rho k) = \nabla \cdot (\rho D_k \nabla k) + G_k + G_b - \rho\epsilon + S_k \tag{6}$$

$$\frac{D}{Dt}(\rho\epsilon) = \nabla \cdot (\rho D_\epsilon \nabla\epsilon) + \frac{C_1\epsilon}{k}(G_k + C_3 G_b) - C_2 \rho\frac{\epsilon^2}{k} + S_\epsilon \quad (7)$$

$$v_t = C_\mu \frac{k^2}{\epsilon} \quad (8)$$

Where
$\frac{D}{Dt}(\rho k)$ is the mean-flow material derivative of turbulent kinetic energy (local derivative + advection)
$\nabla \cdot (\rho D_k \nabla k)$ is the turbulence transport of k
$\rho\epsilon$ is the dissipation of k
G_b is the buoyancy flux
S_k is the average rate-of-strain tensor with modulus

2.3.2 Modified k-epsilon model equations (applied in OpenFOAM)

Modified k-epsilon model equations incorporate the effect of Rapid Distortion Theory (RDT), but exclude the buoyancy factor, G_b. Its default values of model coefficients are similar as the standard k-epsilon model equations, but with addition of the coefficient $C_{3,RDT}$. Table 1 shows the default values of model coefficients of both standard or modified version k-epsilon model equations. Eqs. (9) and (10) shows the equations of the modified k-epsilon model, which are the equation of k and equation of ϵ respectively [25].

Table 1
The default value of the coefficients of k-epsilon model equations

Coefficients	Value
C_μ	0.09
C_1	1.44
C_2	1.92
$C_{3,RDT}$	0
σ_k	1
σ_ϵ	1.3

$$\frac{D}{Dt}(\rho k) = \nabla \cdot (\rho D_k \nabla k) + G_k - \frac{2}{3}\rho(\nabla \cdot u) - S_k \quad (9)$$

$$\frac{D}{Dt}(\rho\epsilon) = \nabla \cdot (\rho D_\epsilon \nabla\epsilon) + \frac{C_1 G_k \epsilon}{k} - (\frac{2}{3}C_1 - C_{3,RDT})\rho(\nabla \cdot u)\epsilon - C_2 \rho\frac{\epsilon^2}{k} + S_\epsilon \quad (10)$$

2.4 Boundary Conditions

Table 2 shows the boundary conditions (BC) of each parameter of this study using the PIMPLE algorithm and the k-epsilon turbulence model. Dirichlet BC and Neumann BC have been applied alternately at inlet and outlet to optimize the flow continuity and stability [1]. The fixedValue BC was applied at velocity inlet so zeroGradient BC was applied at the velocity outlet to make sure the flow is initiated and being continuous appropriately based on the initial conditions and Navier-Stoke equations. The same goes for the pressure inlet and outlet. However, the pressure inlet was set as zeroGradient while pressure outlet was set as fixedValue to avoid the contradiction between velocity and pressure fields. For turbulence parameters, the inlet BCs specialized for the k-epsilon turbulence model was applied, and zeroGradient was applied at the outlet. Equally important, for velocity and

pressure fields, noSlip BC was applied at the solid wall. For turbulence parameters, the k-epsilon wall function was applied. Uniquely, since an only symmetrical quarter of the elevator system was modeled in this study, symmetry BC was used at the symmetry faces [4].

Table 2
Boundary conditions of each parameter.

	Inlet	Outlet	Car and shaft wall	Car and shaft symmetry region
Velocity, u (m s^{-1})	fixed Value	inlet Outlet	No Slip	symmetry
Kinematic static pressure, p (m^2 s^{-2})	zeroGradient	fixed Value	zeroGradient	symmetry
turbulence kinetic energy, k (m^2 s^{-2})	Turbulent Intensity Kinetic Energy Inlet	inlet Outlet	kqRWallFunction	symmetry
dissipation rate of turbulence kinetic energy, ϵ (m^2 s^{-3})	Turbulent Mixing Length Dissipation Rate Inlet	inlet Outlet	Epsilon Wall Function	symmetry

3. Results and Discussion

Figures 2, 3, 4 and 5 show the development of 10 m s^{-1} airflow until a relatively stable state. These figures show that the airflow was blocked by the large cross-sectional area of the car, separated into two sides, and squeezed to passes through the narrow gap between the shaft and car side wall, from the upstream end (base) of the car until the downstream end (top) of the car. The car's blockage effect and Bernoulli effect causes the air velocity immediate upstream of the car decreased, air velocity within the narrow gap increased, and air velocity downstream the car decreased as shown in Figures 2 and 6 (a). This phenomenon was also reported by a similar study [28]. Conversely, the kinematic static pressure immediately upstream of the car increased, air velocity within the narrow gap decreased, and air velocity downstream the car increased as shown in Figure 3. The same observations were reported by similar past studies [4,9,18]. When the cross-sectional area decreases, the airflow velocity and static pressure increase and decrease respectively under the constant force [29]. The Bernoulli's principle can be applied in this study since the airflow is at a high speed and within a large cross-sectional area wind tunnel, with lower viscosity effects.

The airflow disturbance creates the turbulence eddies, with increasing size of the turbulent wake region located downstream of the car (blockage of the flow). This turbulent wake region has a lower velocity magnitude but higher velocity fluctuation (turbulence). Nonetheless, in Figures 2 and 3, fluctuation in velocity and pressure field of the airflow was observed even after reached the relatively stable state. This is caused by the persisting turbulent eddies within the airflow especially in the wake region. The same phenomenon was reported by Timo [1]. Based on Figure 4, the turbulence kinetic energy increases with the flow development due to the increasing velocity and its fluctuations. Based on Figure 5, the dissipation rate of turbulence kinetic energy, ϵ do not show significant changes, it is relatively higher at the region between the lower side wall of the car and the shaft during the early time but remain relatively constant at a lower value until the end of the simulation. This is because initially when the flow is developing and not stable, the turbulence kinetic energy was used to fluctuate the viscous stresses that resist the change of the fluid by the fluctuating strain rates. After the flow reached its constant velocity and was fully developed with a larger turbulence or eddy length

scale, the loss of its turbulence kinetic energy became negligible compared to its high turbulence kinetic energy [23].

Insight into the turbulence aspect and turbulence model used, as the air velocity and Reynolds number increase, small eddies are produced in the airflow. However, this spatially (small size) and temporally (exist only for short period) small scale oscillations is computationally not worth to be resolved using ordinary Navier-Stokes equation, since the airflow velocity (u) over time has only small local oscillations (u') that can be solved in a time-averaged way, which is less computational costly. Moreover, these small local oscillations appear only in the wake region, instead of the high air velocity region that is significant to be studied [11]. So RANS was used in most of the studies to average up the air velocity along with the simulation time steps, assuming the simulation period is sufficiently long to capture the turbulent fluctuations. Based on Figures 4 and 5, the simulated results show only medium size eddies, showing a smaller wake region and high-velocity region. The same results were reported by the studies using RANS k-epsilon by Li-qun *et al.,* [14], as well as RANS k-omega by Wang *et al.,* [9] and Ling *et al.,* [4]. This simulation approach is sufficient for the study that aims to study the average flow patterns and parameter values as an initial guess to guide the experimental study. For the studies simulated using the DES, all sizes of eddies were simulated, showing a larger wake region and high-velocity region due to a higher fidelity especially for the near-wall region Nishant Singh *et al.,* [16]. This type of simulation approach is required for the studies that aim to simulate all sizes of eddies and focus at the near-wall region, which will then be validated by experimental study.

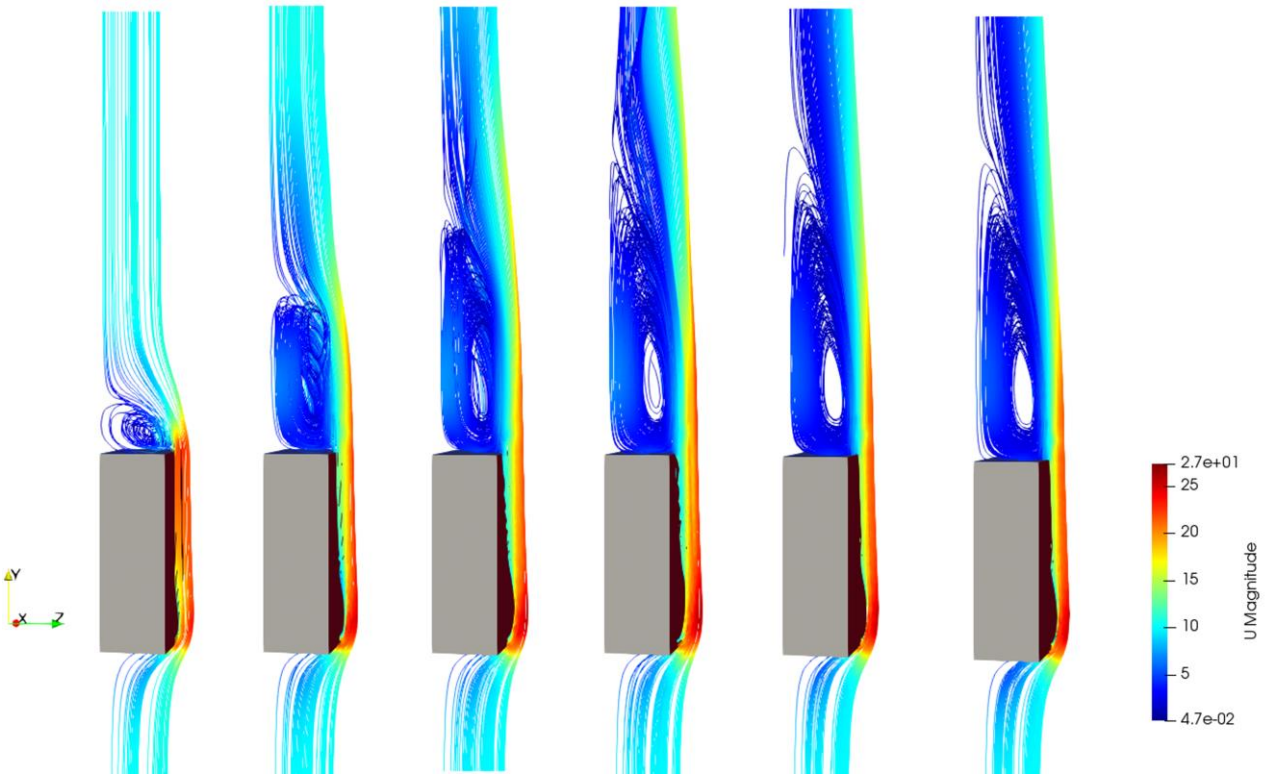

Fig. 2. Streamline plot of the velocity field from the first until the last time steps of simulation

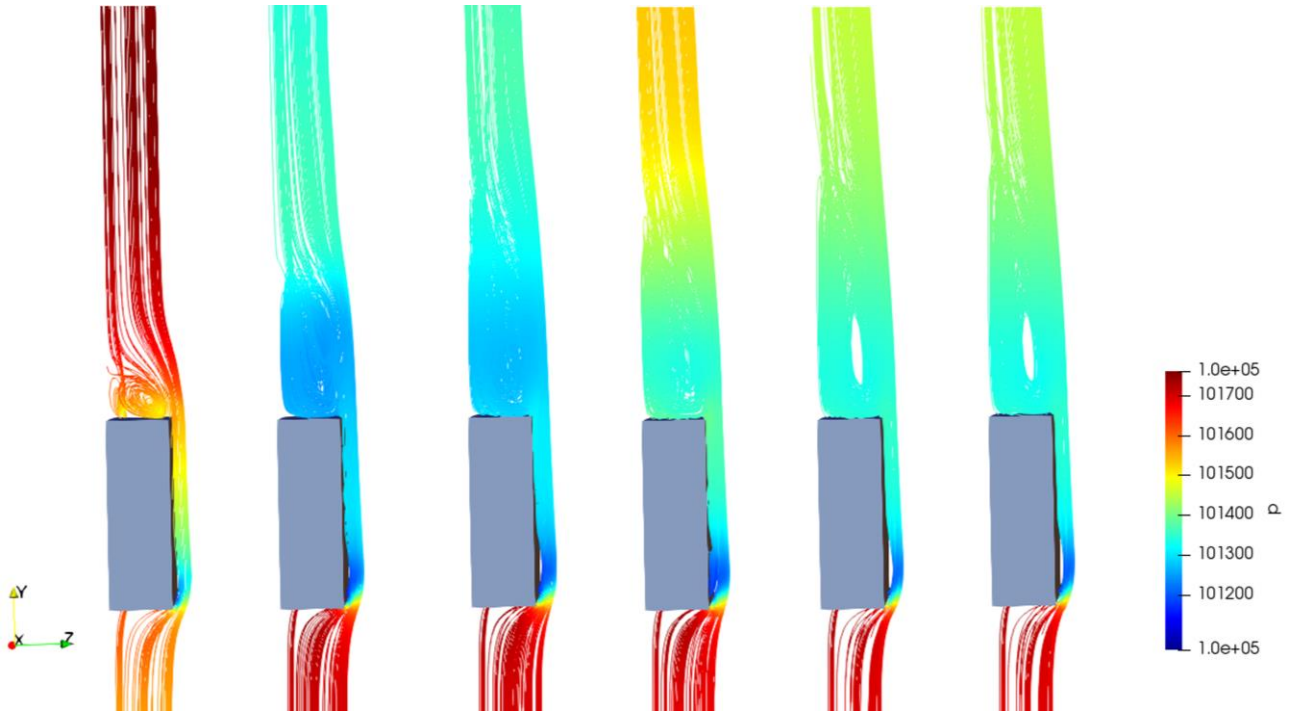

Fig. 3. Streamline plot of the kinematic static pressure field from the first until the last time steps of simulation

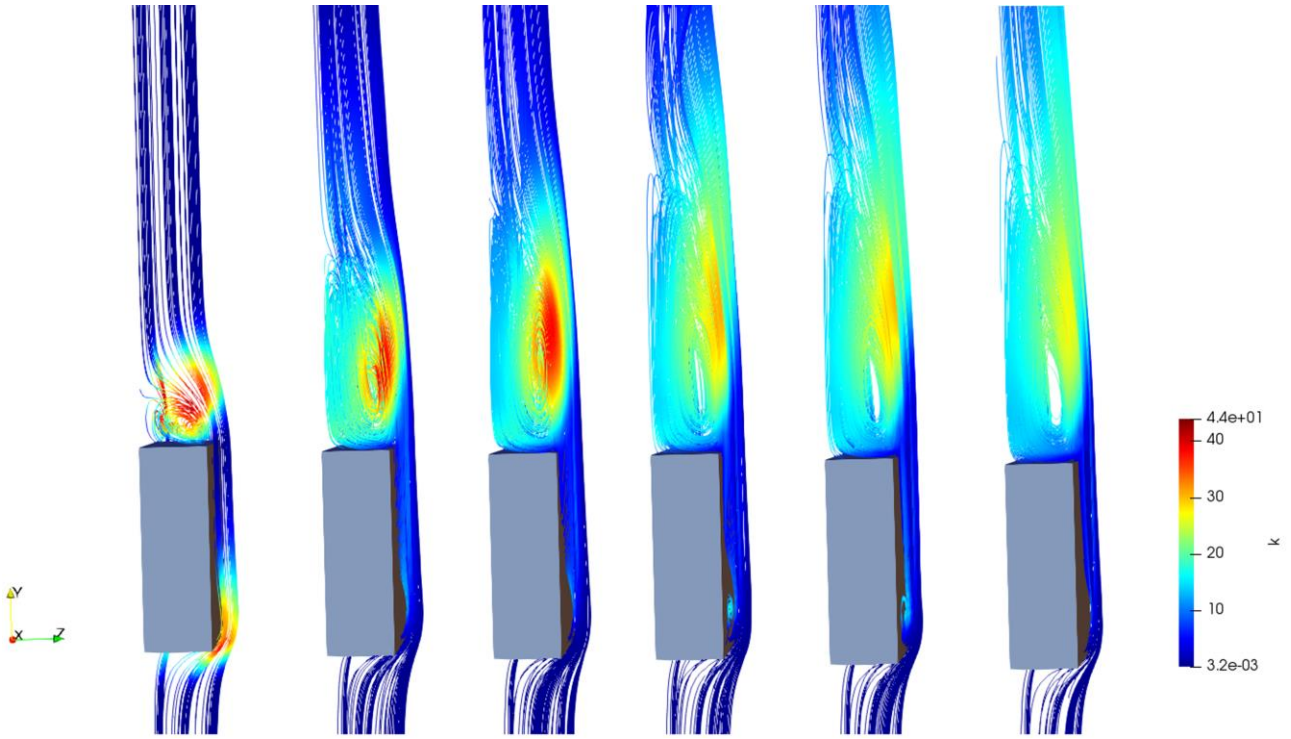

Fig. 4. Streamline plot of the k field from the first until the last time steps of simulation

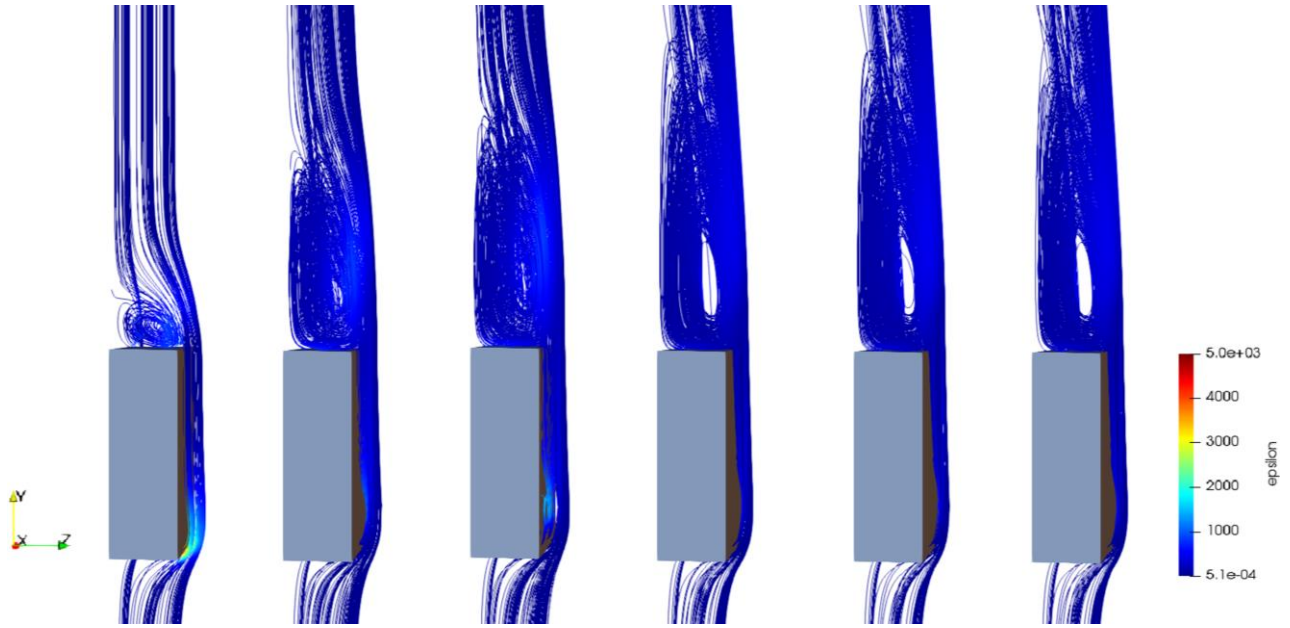

Fig. 5. Streamline plot of the ϵ field from the first until the last time steps of simulation

Figure 6 (a) shows the velocity contour during the stable state of the airflow, with its range of the airflow velocity in directions x, y, and z from 0.0470384 to 27.3158 m s^{-1}. The airflow velocity gradient from the car wall to the distant air in x and z direction was caused by the no slip condition, which was obeyed by all air regardless of the surface roughness. The air velocity decreases when approaching the solid wall [29]. Figure 6 (b) shows the significant measurement points (white dots) for experimental study, which has high velocity and low turbulence. High velocity and low turbulence points can provide a sufficient and stable kinetic energy harvesting.

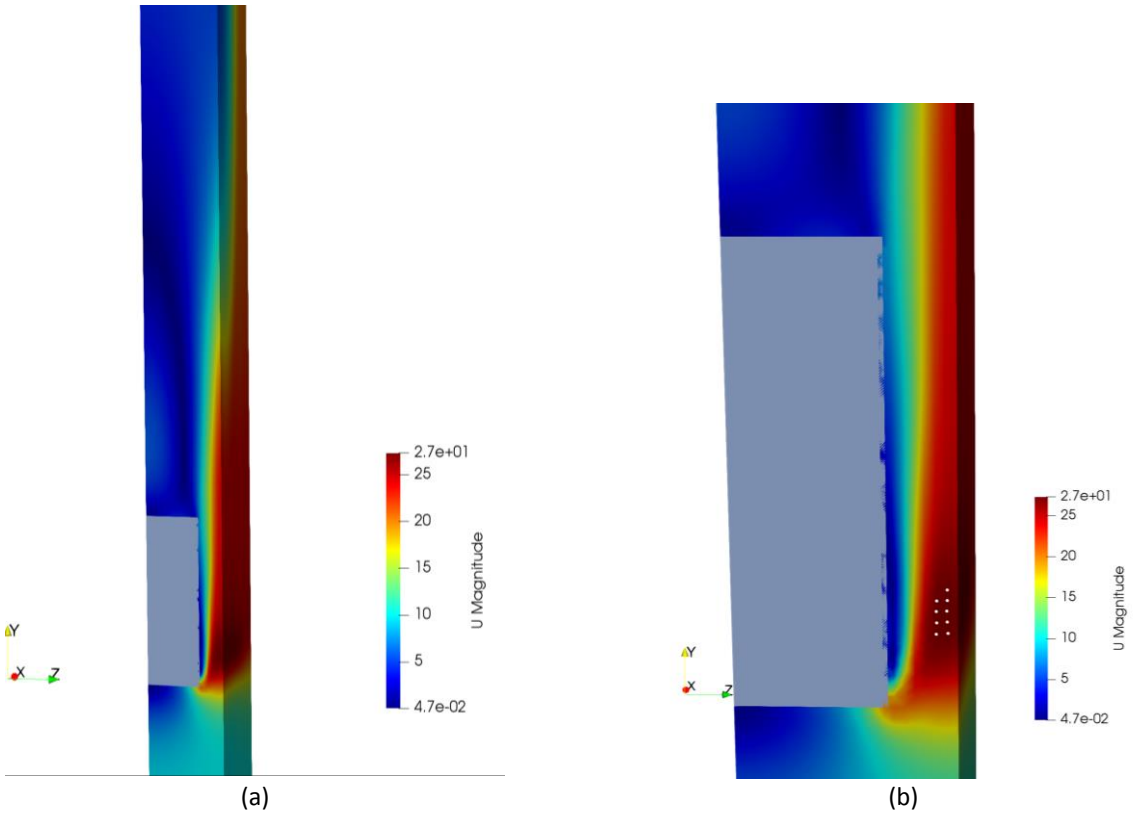

(a) (b)

Fig. 6. (a) Velocity contour of the airflow (b) Points with high velocity and low turbulence

Figure 6 (a) shows the velocity contour during the stable state of the airflow, with its range of the airflow velocity in directions x, y, and z from 0.0470384 to 27.3158 m s^{-1}. The airflow velocity gradient from the car wall to the distant air in x and z direction was caused by the no slip condition, which was obeyed by all air regardless of the surface roughness. The air velocity decreases when approaching the solid wall [29]. Figure 6 (b) shows the significant measurement points (white dots) for experimental study, which has high velocity and low turbulence. High velocity and low turbulence points can provide a sufficient and stable kinetic energy harvesting.

4. Conclusion

Generally, this study discussed the principles and working mechanisms of the PIMPLE algorithm, the k-epsilon turbulence model, as well as the boundary conditions for this approach combination. The airflow surrounding the car was affected by the car's blockage effect and Bernoulli's effect. They were indicated by the flow separation at the bottom wall of the car and flow reattachment at a distant point from the car top (downstream of the wake region), as well as velocity surge and pressure drop at the narrow gap between the car and the shaft respectively. The turbulence of the airflow was observed to increase with the fluctuation of airflow velocity. Overall, the results show a good agreement with the theories of fluid mechanics and physics, as well as the past literature results. Thus, the numerical results are reliable to be used as an initial guess input for further study using the DES approach, as well as reference data for the experimental study. Moreover, significant points with high velocity and low turbulence were determined in order to reduce the unnecessary measurement points in an experimental study.

Acknowledgements

This project is funded by the Trans-disciplinary Research Grant Scheme (TRGS) Ministry of Education Malaysia (203/PTEKIND/67610003) for the financial support in relation to this project. The first author would like to thank Universiti Sains Malaysia (USM) Fellowship scheme for the financial support related to her doctorate study.

References

[1] Timo, Ojanen. "Aero-Vibro Acoustic Simulation of an Ultrahigh Speed Elevator." Tampere University of Technology, 2015.
[2] Zhang, Yang, Xiaowei Sun, Xuefeng Zhao, and Wensheng Su. "Elevator ride comfort monitoring and evaluation using smartphones." *Mechanical Systems and Signal Processing* 105 (2018): 377-390.
[3] Pierucci, Mauro, and Michael Frederick. "Ride quality and noise in high speed elevators." *Journal of the Acoustical Society of America* 123, no. 5 (2008): 3247-3247.
[4] Ling, Zhangwei, Ping Tang, Xuebin Wang, Zheng Lin, and Di Tang. "Research on the drags of high-speed elevator with different height diversion cover." In *2015 4th International Conference on Mechatronics, Materials, Chemistry and Computer Engineering*. Atlantis Press, 2015.
[5] Cai, Weiyong, Zhangwei Ling, Ping Tang, and Zhen Yu Ding. "Optimization design on dome shape of high-speed elevator." In *2015 4th International Conference on Mechatronics, Materials, Chemistry and Computer Engineering*. Atlantis Press, 2015.
[6] Jia Hui Ang, Y Yusup, Sheikh Ahmad, Zaki Shaikh, and Mardiana Idayu Ahmad. "A CFD Study of Flow Around an Elevator Towards Potential Kinetic Energy Harvesting." *Journal of Advanced Research in Fluid Mechanics and Thermal Sciences* 59, no. 1 (2019): 54–65.
[7] Matsuda, Hisashi, Fukuyama Yoshitaka, Yokono Yasuyuki, and Miyasako Kazunori. "The Effect of Car Configurations on the Flow Around Elevator Models (Oil Flow Pattern and Distribution of Pressure Fluctuation on the Model Wall Surface)." In *Flow Visualization VI*, 1992.
[8] Teshima, N., K. Miyasako, and H. Matsuda. "Experimental and numerical studies on ultra-highspeed elevators." *Elevator Technology* 4 (1992): 276-285.
[9] Wang, Xuebin, Zheng Lin, Ping Tang, and Zhangwei Ling. "Research of the blockage ratio on the aerodynamic

performances of high-speed elevator." In *2015 4th International Conference on Mechatronics, Materials, Chemistry and Computer Engineering*. Atlantis Press, 2015.
[10] Greenshields, CJ. "OpenFOAM Foundation User Guide," 2019.
[11] Frei, Walter. "Which Turbulence Model Should I Choose for My CFD Application?" *COMSOL Blog*, 2017, 1–8.
[12] D Scott-Pomerantz, Collen. "The K Epsilon Model in the Theory of Turbulence." University of Puttsburgh, 2004.
[13] K. Rantanen. "Flow Effects on Ride Comfort in Super High Speed Elevators." Helsinki University of Technology, 2002.
[14] Shi, Li-qun, Ying-zheng Liu, Si-yu Jin, and Zhao-min Cao. "Numerical simulation of unsteady turbulent flow induced by two-dimensional elevator car and counter weight system." *Journal of Hydrodynamics, Ser. B* 19, no. 6 (2007): 720-725.
[15] Wu, Renyuan, Zhencai Zhu, and Guohua Cao. "Computational fluid dynamics modeling of rope-guided conveyances in two typical kinds of shaft layouts." *PloS one* 10, no. 2 (2015): e0118268.
[16] Singh, Nishant, Stefan Kaczmarczyk, and Thomas Ehrl. "An analysis of airflow effects in lift systems." In *Lift and Escalator Symposium* 7, (2017): 24. The University of Northampton, CIBSE Lifts Group, LEIA.
[17] Lehtinen, Antti, Gabriela Roivainen, Jukka Tanttari, and Jaakko Ylätalo. "Aero-vibro-acoustic noise prediction for high-speed elevators." In *Akustiikkapäivät 2017*, (2017): 317-322. Akustinen Seura ry.
[18] Mirhadizadeh, Seyed, Stefan Kaczmarczyk, Nathan Tongue, Hayder Al-Jelawy, Peter Feldhusen, W. Delk, K. Anderson, and F. Dudde. "Modelling and computer simulation of aerodynamic interactions in high-rise lift systems." In *Lift and Escalator Symposium* 5, (2015): 117-124. The University of Northampton, CIBSE Lifts Group, LEIA.
[19] Syney Elevator. "Study and Improvement on Aerodynamic of High-Speed Elevator." Syney Elevator, 2014.
[20] Lotfabadi, Pooya. "High-rise buildings and environmental factors." *Renewable and Sustainable Energy Reviews* 38 (2014): 285-295.
[21] DHSS. *Atmosphere and Gas Laws*. 4th ed. Alaska Department of Health and Social Services, 2005.
[22] Mijorski, Sergey, and Stefano Cammelli. "Stack effect in high-rise buildings: a review." *International Journal of High-Rise Buildings* 5, no. 4 (2016): 327-338.
[23] CFD Online. "Introduction to Turbulence / Turbulence Kinetic Energy." Cfd-Wiki, 2018.
[24] CFD-Wiki, Turbulence kinetic energy, CFD-Wiki Turbul. Parameters. (2018).
[25] OpenFOAM Documentation, "K-Epsilon Model Equations OpenFOAM." 2018.
[26] https://en.wikipedia.org/wiki/Turbulence_kinetic_energy.
[27] Jehad, D. G., G. A. Hashim, A. K. Zarzoor, and CS Nor Azwadi. "Numerical Study of Turbulent Flow over Backward-Facing Step with Different Turbulence Models." *Journal of Advanced Research Design* 4, no. 1 (2015): 20-27.
[28] Gilbert, Timothy. "Aerodynamic Effects of High Speed Trains in Confined Spaces." University of Birmingham, 2013.
[29] Alexander, David E. "Fluid Biomechanics." In *Nature's Machines*, 51–97. Elsevier, 2017.